Pictures of the Fractional Quantized Hall Effect

H.L. Störmer

AT & T Bell Laboratories, Murray Hill, NJ 07974, USA

These lecture notes present the basic experimental facts of the integral and fractional quantized Hall effect. By means of a phenomenological comparison between integral and fractional quantized Hall effect, it is concluded that the fractional quantized Hall effect is of many-particle origin. A simplified approach to the presently prevailing theoretical model of the electronic groundstate and its quasi-particle excitations is presented, together with a set of illustrations, in the hope of providing some physical insight into this novel many-particle state.

INTRODUCTION

The essence of the experimental observations, termed the quantized Hall effect, is quickly stated. At low temperatures and in high perpendicular magnetic fields, the Hall resistance ρ_{xy} of a two-dimensional (2D) electron gas is quantized to $\rho_{xy} = h/\nu e^2$ to an accuracy as high as $\sim$ 1 part in 10^7. The quantum number ν can be either an integer (integral quantized Hall effect, IQHE) [1] or a rational fraction with exlusively odd denominator (fractional quantized Hall effect, FQHE) [2]. Concomitant with the quantization of ρ_{xy}, the normal resistivity ρ_{xx} seems to vanish as the temperature tends towards $T = 0$.

Experimental observations of this nature must be surprising even to the most experienced physicists. Traditionally, solid state physics is not the discipline for high-precision measurements of quantum numbers, and yet this phenomenon shows an accuracy which rivals the accuracy of experimental data achieved in atomic physics. (Interestingly enough, an ideal 2D system would not even show the effect; a small amount of randomness is essential). Fractional quantum numbers generally belong to the realm of elementary particle physics, and yet the fractional quantized Hall effect exhibits quantum numbers such as $\nu = 1/3$ and $\nu = 2/5$. Vanishing resistivity, the absence of dissipation, is interesting in itself and promises some kind of ideality of the underlying electronic state.

All these features have a fundamental ring to them and the appearance of Planck's constant h and the electronic change e make the quantized Hall effect a macroscopic quantum phenomenon.

These lecture notes restate the basic observations of the IQHE and the FQHE. The IQHE is being derived in terms of the single-particle density of states of a 2D electron system in a magnetic field. From a phenomenological comparison between the IQHE and the FQHE it is concluded that the FQHE is of many-particle origin. These parts of the lecture notes are a reiteration of an earlier review [3]. In a final chapter, the presently prevailing theoretical model for the electronic groundstate and its quasi-particle excitations are presented. Though the approach is not rigorous, it is hoped that this train of thought and the accompanying illustrations might help the reader to develop an intuitive understanding of this novel, highly correlated electronic state. For these lecture notes no attempt is being made to present a complete listing of citations. For this purpose we refer the reader to a few recent review articles and lecture notes listed at the end.

1. Two-Dimensional Systems.

Two-dimensionality of the electronic system is an important prerequisite for the observation of the QHE. This first chapter briefly reviews the classical device structures in which these conditions can be achieved [4].

In a three-dimensional world two-dimensional (2D) systems are necessarily associated with a surface or an interface. The motion of a particle along the plane (x,y) is essentially free, while its normal motion is restricted. For quantum mechanical objects these restrictions can be made so severe that the particle loses any degree of freedom in the z-direction, and hence assumes a truly 2D character. This situation is achieved by confining the particle to a narrow potential well in the z-direction. Quantum mechanically, the bound states of such a potential well are discrete, with a typical energy spacing of

$$\Delta E \sim \frac{\hbar^2}{2m^*}\frac{1}{d^2} \sim 10 \text{ meV} \qquad (1)$$

(for a well width $d \sim 50\text{Å}$ and $m^* \sim 1/10 m_e$ typical for electrons in semiconductors). At low temperatures ($kT \ll \Delta E$) carriers trapped in the lowest bound state of such a well lack any degree of freedom in the z-direction, while being able to move freely along the interface following the free-particle dispersion relation

$$E = \frac{h^2 k_{xy}^2}{2m^*} \qquad (2)$$

Two devices are presently preferred to generate 2D carrier systems. In a Si-MOSFET, carriers are confined to the interface between Si and SiO_2 via a strong electric field establishing a quasi-triangular potential well [4] (Fig. 1).

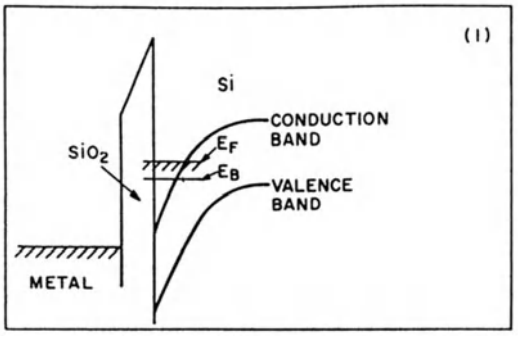

Fig.1 Carrier confinement in a Si MOSFET. A quasi-triangular potential well is established via the Si-SiO_2 interface and an external voltage which is applied to the gate metal.

The second structure is termed modulation-doped GaAs-(AlGa)As heterostructure, in which the equivalent situation is achieved by an abrupt doping profile, resulting in carrier confinement at the GaAs-(AlGa)As interface [3] (Fig. 2). The Si-MOSFET has the advantage over GaAs-(AlGa)As that the 2D carrier concentration can readily be varied by the application of an external gate-voltage. Conversely, the mobility μ of carriers in the GaAs-(AlGa)As ($\mu \sim 10^6$ cm^2/Vsec) far exceeds those of carriers in a Si-MOSFET ($\mu \sim 10^4$ cm^2/Vsec). Since a low carrier scattering rate is crucial for the observation of the FQHE the GaAs-(AlGa)As system is presently preferred for studies of this kind.

2. Integral Quantum Hall Effect (IQHE) in Modulation-Doped Systems

This chapter describes some aspects of the integral quantum Hall effect (IQHE) as it is observed in modulation-doped GaAs-(AlGa)As and thereby introduces some of the notation used in the next chapter. Figure 3 shows one of the most distinct

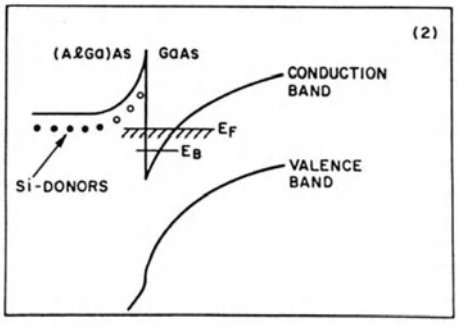

Fig.2 Carrier confinement in a modulation-doped GaAs-(AlGa)As heterojunction. A quasi-triangular potential well is established via the GaAs-(AlGa)As interface and a strong electric field generated by an abrupt doping profile and subsequentcharge-transfer.

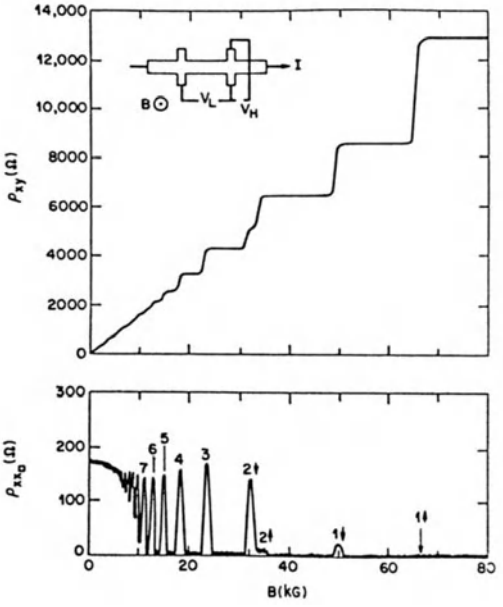

Fig.3 The integral quantum Hall effect IQHE. Low-temperature Hall resistance ($\rho_{xy} = V_H/I$) and magneto-resistance ($\rho_{xx} = V_L/I$) of a modulation-doped GaAs-(AlGa)As sample with a density of n = 4.0×10^{11} cm^{-2} and μ = 8.6×10^4 $cm^2/Vsec$. Insert shows sample configuration [5].

manifestations of the IQHE in a GaAs-(AlGa)As heterostructure at 50 mK [5]. The sample configuration is shown as an insert. Two characteristic voltages V_H and V_L are measured as a current I is imposed onto the 2D system and the perpendicular magnetic field B is varied. V_H, the Hall voltage across the current path, and V_L, the longitudinal voltage along the current path, are normalized to I. This yields the components of the resistivity tensor $\hat{\rho}$ with $\rho_{xy} = V_H/I$ and $\rho_{xx} = gV_L/I$ where g is a geometry factor typically of the order of 1. The relations between the components of the resistivity tensor $\hat{\rho}$ with $\rho_{xy} = V_H/I$ and $\rho_{xx} = gV_L/I$ where g is a geometry factor typically of the order of 1. The relations between the components of the resistivity tensor $\hat{\rho}$ and the components of the conductivity tensor $\hat{\sigma} = \hat{\rho}^{-1}$ are :

$$\sigma_{xx} = \frac{\rho_{xx}}{\rho_{xx}^2 + \rho_{xy}^2}, \quad \sigma_{xy} = \frac{-\rho_{xy}}{\rho^2_{xx} + \rho^2_{xy}}, \quad \sigma_{yy} = \sigma_{xx}, \quad \sigma_{yx} = -\sigma_{xy} \tag{3}$$

$$\rho_{xx} = \frac{\sigma_{xx}}{\sigma_{xx}^2 + \sigma_{xy}^2}, \quad \rho_{xy} = \frac{-\sigma_{xy}}{\sigma^2_{xx} + \sigma^2_{xy}}, \quad \rho_{yy} = \rho_{xx}, \quad \rho_{yx} = -\rho_{xy} \tag{4}$$

At first glance these equations seem to be surprising, since vanishing resistivity ($\rho_{xx} \to 0$) implies also vanishing conductivity ($\sigma_{xx} \to 0$), while in the absence of a magnetic field one quantity is the inverse of the other. Figure 4 illustrates this

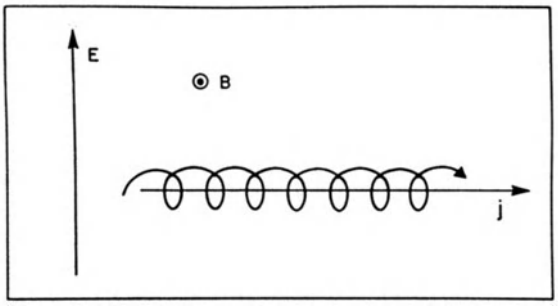

Fig.4 Cycloid motion of a carrier in crossed electric (E) and magnetic fields (B).

counterintuitive relationship for carriers in a crossed magnetic (B) and electric field (E). Under such conditions carriers move on a cycloid orbit in the direction perpendicular to E and B. Since there is no electric current along E the conductivity $\sigma = i/E = 0$. Conversely, the absence of any electric field component along the current direction implies for the resistivity $\rho = E/j = 0$.

From purely classical considerations, i.e., balancing the Lorentz force acting on a carrier moving in a magnetic field against the force from the electric Hall field, it is expected that ρ_{xy} shows a linear magnetic field dependence

$$\rho_{xy} = B/en \tag{5}$$

with n being the 2D electron density. Rather than this linear B-dependence, Fig. 3 shows a Hall resistivity ρ_{xy} which assumes a staircase-like structure with plateaus quantized to

$$\rho_{xy} = h/ie^2 \ , \ i = 1,2,3... \tag{6}$$

The accuracy of this quantization has been verified to approximately 1 part in 10^7. Concomitant with the appearance of plateaus in ρ_{xy}, the diagonal resistivity ρ_{xx} seems to vanish over large portions of B. Resistivities as low as $\rho_{xx} < 10^{-10}\ \Omega/$ equivalent to roughly $10^{-16}\ \Omega$ cm, have recently been established.

Following the present understanding of the IQHE,the formation of plateaus in ρ_{xy} and vanishing values of ρ_{xx} are directly related to the singularities in the density of states (DOS) of a 2D system in a strong perpendicular magnetic field (Fig. 5a). The DOS of an ideal two-dimensional system consists of spin-split Landau levels with energies

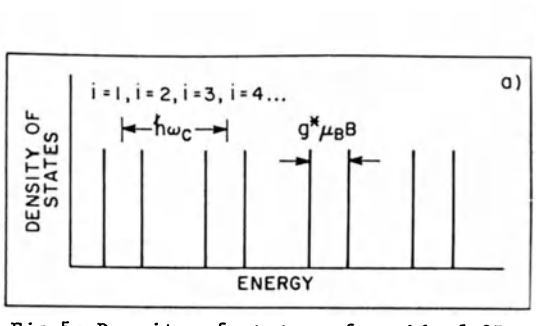

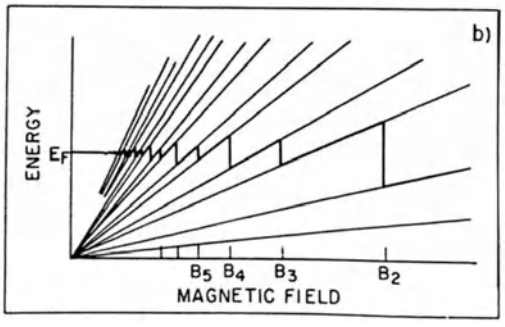

Fig.5a Density of states of an ideal 2D system. $\hbar\omega_c$ = Landau splitting, $g^*\mu_B B$ = spin splitting. The degeneracy of each singularity is $d = eB/h$.
Fig.5b Landau fan and position of Fermi energy E_F as a function of field for an ideal 2D system at low temperature.

$$E = (j + 1/2)\hbar\omega_c \pm Sg^{\cdot}\mu_B B, \quad j = 0,1,2... \tag{7}$$

$\hbar\omega_c = \hbar eB/m^{\cdot} = 0.17$ [meV/kG]xB is the Landau level splitting for an effective mass of GaAs of $m^{\cdot} = 0.067\ m_o$. S is the spin of the carriers, $g^{\bullet}$ their effective g-factor and $\mu_B = eh/2m_o$ is Bohr's magneton. For our purposes it is not important to discern between Landau level splitting and spin-splitting. We only retain a sequence of singularities (from now on called magnetic levels or levels) numbered by i = 1,2,3 ... starting with i = 1 at the lowest energy. The number of states per level for any 2D-system is

$$d = eB/h = B/\Phi_o = 2.42 \times 10^9\ cm^{-2}\ kG^{-1} \times B \tag{8}$$

where $\Phi_o = h/e$ is the magnetic flux quantum. This value is independent of any material parameter. Through it one can define a filling factor

$$\nu = n/d. \tag{9}$$

At low temperatures($kT \ll \hbar\omega_c$, $g^{\cdot}\mu_B B$) and at any given field, ν indicates the number of populated levels. Noting that n is the number of carriers per unit area and d is the number of flux quantum per unit area, ν is also a measure of the number of flux quantum associated with each electron. For a system with fixed carrier density, the filling factor decreases as B is raised. The variation of the Fermi level E_F is periodically abrupt due to the strongly singular DOS (Fig. 5b). At any given field, E_F resides in the close vicinity of level i = int (ν) + 1. However, an exceptional situation arises at fields

$$B_1 = n\ \Phi_o/i \tag{10}$$

where an exact multiple i of levels is filled. Then E_F is intermittent and lies in the gap region between level i and level i + 1.

The value of ρ_{xy} and the vanishing of ρ_{xx} can then be derived apparently in the following way : The diagonal conductivity σ_{xx} is entirely dependent on the DOS at the position of E_F. Since the DOS vanishes in the gap region, σ_{xx} vanishes as well and with Eq. 4 we derive $\rho_{xx} = 0$ as long as $\rho_{xy} \neq$. The classical expression $\rho_{xy} = B/en$ holds also for quantum mechanical free electrons. Hence, at a sequence of singular points on the field axis $B_1 = n\Phi_o/i$ where ρ_{xx} vanishes, the Hall resistance is $\rho_{xy} = \Phi_o/ie = h/ie^2$.

Such a derivation of ρ_{xx} and ρ_{xy} neither accounts for the finite width of the plateaus nor for the width of the zero resistance regions,both of which are the truly outstanding features of the IQHE. Explanation of a finite width of these

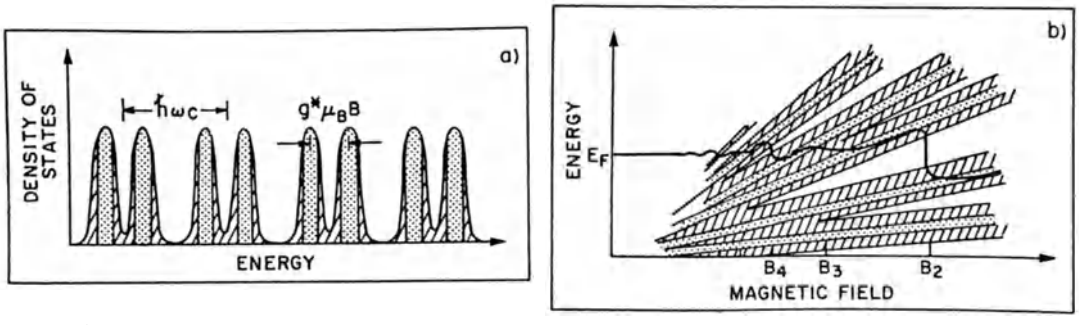

Fig.6a Density of states of a real 2D system. Disorder broadens the singularities (Fig.5a) into bands. The central part of each band contains delocalized states while the states in the flanks are localized, not participating in transport.
Fig.6b Landau fan and position of Fermi energy E_F as a function of field for a real 2D system at low temperature.

features requires the existence of localized states. Localized states are expected to be present in real two-dimensional systems, due to disorder as a result of random distribution of impurities or random interface steps. They lift the degeneracies of the magnetic levels and broaden them (Fig. 6a). States at the center of this distribution will be extended, while those in its tails will be localized, not participating in electronic transport. This broadening of the magnetic levels moderates the abrupt jumps of E_F from one level to the next as B is varied about the crucial values B_1 (Fig. 6b). Hence, for finite ranges of field, E_F moves through regions of localized states between magnetic levels. In an elegant gedanken experiment [6] LAUGHLIN has shown that under these conditions ρ_{xy} remains quantized and ρ_{xx} tends towards zero in spite of the disorder. He demonstrates quite generally that independent of the strength of the disorder

$$\sigma_{xx} = 0 \text{ and } \sigma_{xy} = ie/\Phi_o = ie^2/h, \quad i = 0, \pm 1, \pm 2... \tag{11}$$

whenever E_F lies within localized states (mobility gap) or within the region of a true gap. The value of i may be zero, which describes the case of an insulator. Except for this degenerate case i is finite and, hence, with Eq. 4

$$\rho_{xx} = 0 \text{ and } \rho_{xy} = h/ie^2, \quad i = 0, \pm 1, \pm 2... \tag{12}$$

which are the quantities one generally obtains in transport measurements. The quantized region may be wide (as wide as 95% plateaus and 5% transitions) indicating that the major part of the DOS consists of localized states and still Eq. 12 holds. LAUGHLIN's gedanken experiment does not specify the value of i. For weak disorder i is expected to coincide with the value obtained from the ideal case, in agreement with the experiment.

We summarize this chapter stating that the IQHE is understood in terms of gaps in the single particle DOS of a 2D electron system in a strong perpendicular magnetic field. Disorder leads to the formation of localized states in the gap region between magnetic levels. Whenever the Fermi energy lies in this range $\rho_{xx} = 0$ and $\rho_{xy} = h/ie^2$ (i = 1,2,3...) excluding the degenerate case i = 0 of an insulator. A single-electron picture is sufficient for a description of the IQHE.

3. The Fractional Quantized Hall Effect (FQHE)

Experiment

The availability of low-density 2D modulation-doped heterostructures with unprecedently high mobilities ($\mu \gtrsim 10^6$ cm^2/Vsec) led to magneto-transport studies on GaAs-(AlGa)As structures at low temperatures in extremely high magnetic fields (up to 280 kG) where the extreme quantum limit could be reached. In terms of the filling factor $\nu = n/d$ the extreme quantum limit, where only the lowest magnetic level is populated, is characterized by $\nu \leq 1$. Figure 7 shows ρ_{xy} data from a sample of constant electron density $n = 2.13 \times 10^{11}$ cm^{-2} and mobility $\mu \gtrsim 10^6$ cm^2/Vsec.[7]. For this low concentration, exact multiples ($\nu = i$) of magnetic levels are filled at $B = nh/ie \gtrsim 88$ kG, 44 kG, 22 kG... In the vicinity of these field positions one expects the appearance of the IQHE. The last of these plateaus and concomitant resistance minimum are indeed observed at $B_1 \gtrsim 88$ kG. Data below 70 kG were not accessible, due to the use of a fixed base field from a superconducting magnet. Measurement in the absence of this base field (not shown) reveals clearly the higher orders ($\nu = 2,3...$) of the IQHE. The majority of Fig. 7 covers the region of the extreme quantum limit where $\nu < 1$. Contrary to expectation, a rich sequence of structures is observed, reminiscent of the IQHE. However, the deduced quantum numbers are not integers but rational fractions with exclusively odd denominators. At the present time, structures in ρ_{xx} have been observed in the vicinity of filling factors

$$\begin{aligned} &\nu = 1/3,\ 2/3,\ 4/3,\ 5/3,\ 8/3 \\ &\nu = 1/5,\ 2/5,\ 3/5,\ 4/5,\ 6/5,\ 7/5,\ 8/5 \\ &\nu = 2/7,\ 3/7,\ 4/7 \\ &\nu = 4/9,\ 5/9 \end{aligned} \tag{13}$$

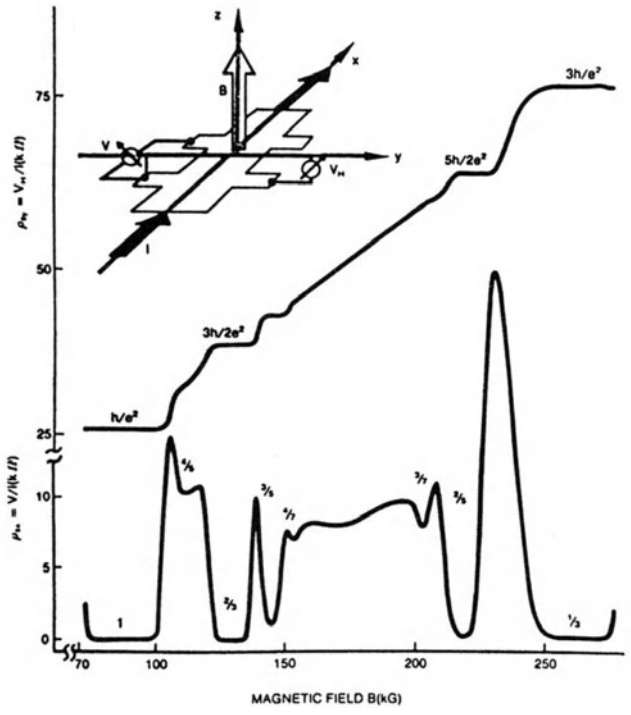

Fig.7 The fractional quantum Hall effect FQHE. Low-temperature Hall resistance ρ_{xy} and magneto-resistance ρ_{xx} of a very high-mobility modulation-doped GaAs-(AlGa)As sample with density $n = 2.13 \times 10^{11}$ cm^{-2} and mobility $\mu \sim 10^6$ cm^2/Vsec in the extreme quantum limit ($\nu < 1$). Structures resembling the IQHE (Fig. 3) occur at fractional filling factor ν. [7].

The concomitant Hall plateaus of the more prominent of these structures have been determined to be quantized to $\rho_{xy} = h/\nu e^2$ to an accuracy as high as 3 parts in 10^5 (limited by the equipment). While the existence of plateaus in ρ_{xy} and vanishing resistance in ρ_{xx} at integer filling factor ν are well accounted for by the IQHE, the appearance of similar phenomena at fractional ν is inconsistent with such an interpretation. Not only do these structures appear at fractional occupation of a magnetic level but, moreover, ρ_{xy} is quantized to $\rho_{xy} = h/\nu e^2$ with ν being an exact rational fraction and not an integer.

Since phenomenologically these new features resemble those of the IQHE, this phenomenon is termed the fractional quantum Hall effect (FQHE), though both must be of different origin. While the IQHE can be explained in terms of non-interacting 2D electrons in a high magnetic field, no such interpretation seems to be possible for the FQHE.

4. Phenomenological interpretation of the FQHE

In order to assess the possible origin of the FQHE, we return to Laughlin's gedanken experiment described in section 2. As an example, we choose the $\nu = 1/3$ state. The other fractions can be discussed in an analogous way. From $\rho_{xx} \sim 0$ and $\rho_{xy} \neq 0$ at $\nu \gtrsim 1/3$, we can deduce $\sigma_{xx} \to 0$. Hence, the DOS at the position of E_F for partial filling of the lowest magnetic level is vanishingly low, being either zero and forming a true gap, or finite but localized, forming a mobility gap.

The appearance of such gaps in the single particle DOS of 2D electrons in the extreme quantum limit is totally unexpected. A description of the minima in ρ_{xx}

cannot be given in terms of a non-interacting particle DOS. One has to involve electron interaction for their explanation.

The formation of the long predicted electron Wigner solid, where a finite gap separates the condensed state from the single particle excitations, initially seems to provide a basis for the observed anomalies. This would require such an electron solid to form preferentially around given filling factors, e.g. $\nu = 1/3$. Numerical studies on the groundstate energy of a Wigner solid and the related CDW in a 2D system in the extreme quantum limit indicate no preference for any given fractional ν and, hence, call in question any interpretation of the FQHE in terms of A Wigner solid. Experimental data also dismiss such an interpretation. At low temperature, and in the presence of disorder, a Wigner lattice is pinned to potential fluctuation and a non-linear current/voltage characteristic is expected to occur as the solid becomes depinned at small electric fields. Measurements at $\nu = 1/3$ down to electric fields as low as 10 μV/cm did not produce any such non-linearities.

Since a Wigner solid does not seem to explain the experimental results, we must look beyond such an interpretation. For this we return to the earlier gedanken experiment, which requires $\rho_{xy} = h/ie^2$, $i = \pm 1, \pm 2, \ldots$ whenever E_F lies in a gap region (excluding here the trivial case $i = 0$). The experimental result $\rho_{xy} = h/1/3\ e^2$ is clearly in conflict with such a conclusion, indicating that the assumptions under which the statement was derived do not hold for the electronic state responsible for the FQHE. However, with an ad hoc assumption, Eq. 12 can be reconciled. This will shed some light on the possible nature of the underlying electronic state.

Laughlin's gedanken experiment [6] relies on gauge invariance of the vector potential (by which the flux quantum Φ_o enters the derivation of ρ_{xy}), and on the quantization of the electric charge, e. The final result is actually stated as a ratio of these quantities $\rho_{xy} = \Phi_o/ie = h/ie^2$. The experimentally observed value of $\rho_{xy} = \Phi_o/\ 1/3\ e$ in the FQHE can be regained if we assume the formation of carriers with effective fractional charge $e^* = 1/3\ e$.

Fractionally charged quasi-particles as current-carrying units, and the existence of a gap at E_F for $\nu = p/q$ do provide a phenomenological explanation of the FQHE with $\rho_{xy} = \Phi_o/e^*$. The above deduction is by no means rigorous. This picture is rather brought forward here, guided by recent theoretical studies on the groundstate of 2D systems in the extreme quantum limit, which suggest the formation of a novel electron liquid with fractionally charged quasi-particles of fraction ν.

5. Present Understanding of the FQHE

This chapter retraces the lines of thought which led to the presently prevailing theoretical model for the electronic state underlying the FQHE.

The discovery of the FQHE has initiated a reexamination of the groundstate of a 2D electron system in the extreme quantum limit. A numerical calculation by YOSHIOKA, HALPERIN and LEE [8] for a finite size system of 4, 5, and 6 electrons in a rectangular box with periodic boundary conditions in a high magnetic field, yielded three important results :

1. Over a wide range of ν, the groundstate of the collection of electrons is significantly lower than that of a Wigner solid.
2. At $\nu = 1/3$ (and possibly at $\nu = 2/5$, but also at $\nu = 1/2$), the groundstate energy, as a function of ν, develops a downward cusp, indicating a commensurate energy at these filling factors.
3. The pair correlation function of the groundstate differs considerably from that of a Wigner crystal.

All these results indicate that the Wigner crystal is not the groundstate for this finite system. While extrapolation to many electrons is unreliable, these numerical data, nevertheless, are suggestive for the groudstate of a real system.

An analytic expression for the groundstate of a 2D system in the extreme quantum limit at rational filling factor was recently proposed by LAUGHLIN [9]. This many-particle wavefunction, with built-in-pair correlation, presently forms the basis for most theoretical models of the FQHE.

LAUGHLIN's wavefunction has the following properties :

1. It describes a state which only has a filling factor $\nu = 1/m$, where m is an integer. Assuming electron/hole symmetry, a case can also be made for $\nu = 1 - 1/m$.
2. It is antisymmetric only for odd m, hence, only odd denominators are allowed.
3. Its pair correlation function suggests it to be a novel quantum-fluid rather than a Wigner solid for $m \lesssim 10$.
4. The elementary excitations are separated from the groundstate by a finite gap.
5. These quasi-particle excitations have fractional charge $e^* = e/m$.
6. The quantum-fluid is incompressible and has no low-lying excitations. Hence, it flows resistance-less at T = 0.
7. For $m \gtrsim 10$, the quantum liquid is expected to crystalline into a Wigner solid.

For a rigorous derivation of these properties I refer the reader to the original literature and to some recent review articles on the subject.

5.1 Illustration of the Wavefunction

In the remainder of the paper I would like to present a greatly simplified approach to Laughlin's wavefunction. Though it lacks rigor it might assist the reader in developing a physical understanding of the electronic state at fractional filling of a Landau level. The lines of thought follow closely a suggestion by Halperin [10].

The wavefunction proposed by LAUGHLIN to describe the state at filling factor $\nu = 1/m$ is :

$$\Psi(Z_1, Z_2 \ldots Z_N) = \prod_{i<j}^{N} (Z_i - Z_j)^m \exp\left[-\frac{1}{4} \sum_k |Z_k|^2 \right] \tag{14}$$

The square of this N-particle wavefunction describes the probability to find the N participating electrons at positions Z_1, Z_2 ... Z_N.

The complex plane has been chosen to represent the 2D plane. Such a choice is a matter of mathematical convenience since it simplifies Eq. 14 considerably. A particle at (x,y) in the real 2D plane is described by a single complex number $z = (x - iy)l_o$ where $l_o = \sqrt{\hbar/Be}$ is the magnetic length. Apart from the scale factor l_o and an inversion of the y-axis, the real 2D plane and the complex plane are equivalent.

Many particle wavefunctions are difficult to visualize. In order to simplify this task we will focus on the motion of one prototype-electron (Z_N) in the presence of all other electrons fixed at positions Z'_1, Z'_2, $Z'_3 \ldots Z'_{N-1}$. The wavefunction for this single particle is then :

$$\Psi(Z_N) = Z_o \exp\left[-\frac{1}{4} |Z_N|^2 \right] \prod_{1}^{N-1} (Z_N - Z'_i)^m \tag{15}$$

where the products over all fixed pairs, $[Z'_i - Z'_j)^m$ and their exponential are collected into Z_o. Equation (15) describes a particle which moves through a set of fixed points Z'_i like a ball through a pin-ball machine trying to stay away from the fixed particles. In the vicinity of each of the fixed electrons its wavefunction decays rapidly with a power m.

It is instructive to try to develop an intuitive understanding of the particular form of Eq. 15. For this we start with a single electron in the lowest Landau level (spin neglected) on an infinite 2D plane in a normal field B restricted to the lowest Landau level. Using a symmetric gauge, its wavefunction can be written as

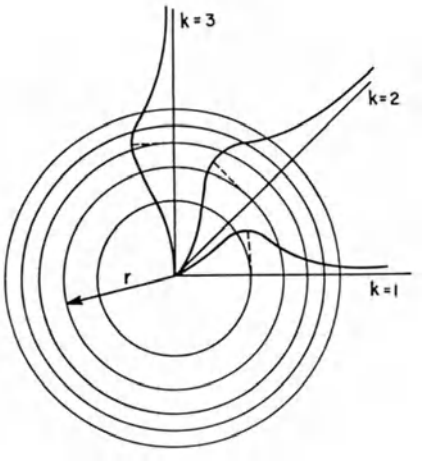

Fig.8 Illustration of the basis functions for a 2D-carrier in the lowest Landau level using a symmetric gauge for the vector potential. The orbits are racetracks about the origin with increasing angular momentum k and increasing radius r = $\sqrt{2k}$ l_o, $l_o = \sqrt{\hbar/Be}$.

$$\phi(Z) = P\, Z^k \exp\left[-\frac{1}{4}|Z|^2 \right] \tag{16}$$

where P is a normalization factor and the same complex notation is used. These wavefunctions are racetracks around the origin with angular momentum k and orbital radius r = $\sqrt{2k}$ in units of l_o (see Fig. 8). The general case of a wavefunction for one electron in the lowest Landau level can then be written as a linear combination of these basic functions

$$\Psi(Z) = P' \exp\left[-\frac{1}{4}|Z|^2 \right] \sum_{k-1} a_k Z^k \tag{17}$$

with expansion coefficients a_k.

If we confine the system to a large dis of radius R (in units of l_o) the basic functions remain approximately valid, but the expansion has to be cut off for orbitals bigger than R. The limits k to $k_{max} = S = R^2/2$.

$$\Psi(Z) = P' \sum_{k-1}^{s} a_k Z^k \exp\left[-\frac{1}{4}|Z|^2 \right] \tag{18}$$

Since the exponential in Eq. 18 is always a positive real number $\Psi(Z)$ has s roots (Z'_1, Z'_2, Z'_3...Z'_s) in the complex plane. Then $\Psi(Z)$ can obviously be expressed in terms of its roots

$$\Psi(Z) = P' \exp\left[-\frac{1}{4}|Z|^2 \right] \prod_{k=1}^{s} (z - z'_k) \tag{19}$$

Though in principle some roots might be degenerate (same position), for a general case they are roughly uniformly distributed over the disc (Fig. 9). On a small loop around each root the phase of the wavefunction changes exactly by 2π. We might call these points vortices due to their formal analogy to vortices in superconductors. Their extent is $\sim \sqrt{2}l_o$ and their density in the plane is $\eta = s/\pi R^2 l_o^2 = Be/h = B/\Phi_o$ which coincides with the density of flux quantum Φ_o due to the magnetic field B.

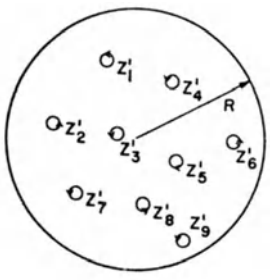

Fig. 9

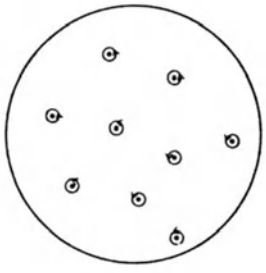

Fig. 10

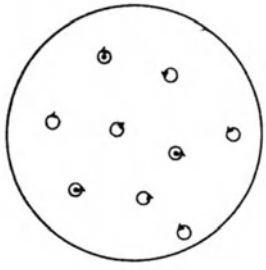

Fig. 11

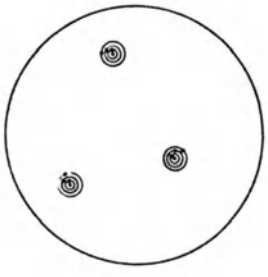

Fig. 12

Ó VORTEX
• ELECTRON

Fig.9 Illustration of a general wavefunction for a single 2D-carrier in the lowest Landau level confined to a large disc of radius R. The z_i' indicate the positions of "vortices" i.e., positions where the wavefunction vanishes and its phase changes by 2π around it. Their density is the same as the magnetic flux density $\eta = B/\Phi_o$ of the magnetic field B.
Fig.10 Additional (fixed) electrons can be positioned only at the vortices of the prototype-electron (ψ = 0) to obey Pauli's principle. At maximum filling the electron density equals the magnetic flux density and hence $\nu = 1$, i.e., the Landau level is completely filled.
Fig.11 At $\nu = 1/3$ the electrons occupy only 1/3 of the vortices. The existence of the other vortices is required by the strengh of B but there is no compelling reason for their actual position.
Fig.12 The $\nu = 1/3$ system can considerably reduce its potential energy by placing a three-fold vortex at the position of each electron. This reduces Coulomb interaction since the wavefunction now vanishes like the 3rd power (three vortices) rather than linearly (one vortex).

So far we have considered only a single electron. Were we to add more electrons to the system, we would have to take products over their wavefunctions, antisymmetrize the product and the problem would become quickly unmanageable. However, we are satisfied with observing the motion of a prototype-electron among a set of other fixed electrons. Such additional (fixed) electrons in Fig. 9 can only be positioned at the location of the vortices of the prototype in order to obey Pauli's principle. Only in the center of the vortices does the wavefunction of the prototype vanish. As we keep adding carriers we fill up all vortices until an electron density η is reached. This is the maximum number of electrons which fit into the lowest Landau level (Fig. 10). Since the electron density equals the magnetic flux density, the filling factor is exactly $\nu = 1$, as required. Hence, within the limits of our model, which keeps S - 1 particles fixed, Eq. 19 describes the state of a noninteracting electron gas at $\nu = 1$. The prototype-electron produces a vortex at the position of all other electrons.

If we were to release the fixed electrons, simple illustrations like Fig. 10 would be impossible. However, one can imagine snapshots where at any time each

electron generates a vortex at the position of each other electron to satisfy Pauli's principle. Then, by induction from Eq. 19, one might suggest the following wavefunction for this many-particle state.

$$\Psi(Z_1,Z_2,Z_3 \ldots Z_3) = P^H \prod_{|<|}^{s} (z_i - z_j) \exp \sum_{k}^{s} \left[-\frac{1}{4} |z_k|^2 \right] \qquad (20)$$

Indeed, Eq. 20 is the totally antisymmetrized solution for the $\nu = 1$ state in very high magnetic fields neglecting electron-electron interaction.

Our aim, however, is to find an intuitive solution to the $\nu = 1/m$ state. As a concrete example we chose $\nu = 1/3$ and return to Fig. 9. At $\nu = 1/3$ the lowest Landau level is only filled to 1/3 capacity i.e., the fixed electrons occupy only 1/3 of the vortices leaving 2/3 of the vortices unoccupied (Fig. 11). Vortices at the position of the fixed electrons are required by the Pauli principle. There are no compelling reasons for vortices at other positions, except that the total vortex-density has to remain η. In an interacting system such unoccupied vortices are actually wasteful, since the prototype electron avoids certain points in the plane without gaining energy. A much more favorable solution is to generate three-fold vortices at the position of each fixed electron (Fig. 12). This keeps the prototype further away from the fixed electrons and, hence, reduces considerably the Coulomb energy of the system. Since each fixed electron is located at a three-fold root of ψ this state is just the illustration of Eq. 15 for $m = 1/\nu = 3$. Through induction we regain Eq. 14 which is Laughlin's wavefunction for the electronic state underlying the FQHE. In this state each electron generates an m-fold vortex around each other's electron. Because the wavefunction drops off like the distance between carrier pairs to the m-th power, such a configuration considerably reduces the Coulomb energy of the 2D system. This is the reason why this highly correlated motion of the carriers is energetically so favorable and is believed to form the groundstate of a 2D electron system in a magnetic field.

5.2 Illustration of the Quasi-particles

Excitation from the groundstate of Eq. 15 forms quasi-particles with fractional charge $e^* = e/m$. This section proposes a gedanken experiment to develop an intuitive picture of such an e/3 quasi-particle.

Figure 13 shows again the $\nu = 1/3$ electronic state. There are four fixed electrons each accompanied by a three-fold vortex of the prototype-electron. The extent of each three-fold vortex is $\sim \sqrt{2m}l_o = \sqrt{6}l_o$ which coincides with their average spacing. In this sense the vortices are dense in the 2D plane. The probability of finding the prototype-electron is shown as contour lines tending towards zero in the vicinity of the fixed carriers.

At fixed carrier density we slightly raise the magnetic field so that exactly one more flux quantum Φ_o enters the system. This requires one more single vortex in the wavefunction of the prototype which we might place in the center of Fig. 13. Such an additional vortex requires the wavefunction to vanish at a given point, introduces considerable distortion and raises the total energy of the system. Predominantly this energy increase is caused by the increased cyclotron energy ($1/2\ \hbar\omega_c$). However, a small fraction of it is due to the close proximity of the additional vortex to the neighboring three-fold vortices. It is energetically advantageous for the system to open the cage surrounding the single vortex at the cost of lowering the average distance between all fixed particles and their accompanying three-fold vortices.

In a gedanken experiment we can perform this flux quantum addition three times, creating a three-fold vortex in the center and successively displacing the surrounding carriers. Finally we take an electron from outside the system and place it at the position of the vortices. The resulting state is again a $\nu = 1/3$ state where each fixed electron is associated with a three-fold vortex. This state is

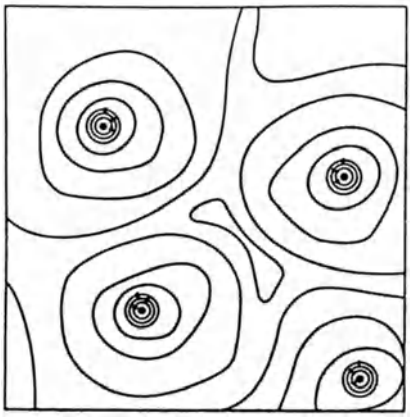

Fig.13

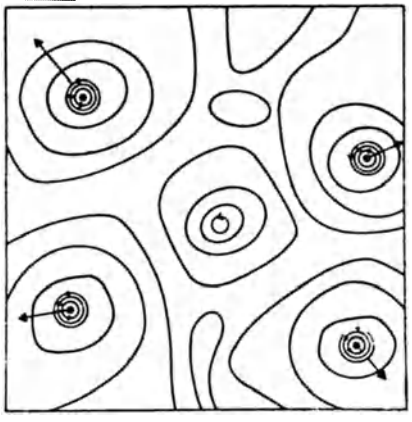

Fig.14

Fig.13 Schematic illustration of $\nu = 1/3$ state. Four electrons are fixed. One electron moves and generates three vortices at the position of each of the fixed electron. Its probability distribution is shown as contour lines tending towards zero near the fixed electrons.

Fig.14 Introduction of one additional vortex (slight increase of magnetic field) into the state of Fig. 13. The vortex considerably perturbs the system. It regains equilibrium by a slight displacement of the fixed carriers. The vortex represents a quasi-particle with charge $e^+/3$.

electrically neutral, since the total charge of the electrons is compensated by the total charge of ionized impurities from which the electrons emerged. Therefore, removing again the additional electron creates locally an apparent positive charge e^+ at the position of the three-fold vortex in the center. With further removal of two of its three vortices, an apparent positive charge of roughly $e^+/3$ will remain i.e., each single vortex in the system appears to be associated with a charge $e^\bullet = e^+/3$. The vortex in the center of Fig. 14 therefore represents a quasi-particle of charge $e^+/3$. They are stable objects and like real carriers these quasi-particles can move through the system carrying a fraction of a charge from one place to another and, hence, give rise to an electrical current. A rigorous calculation shows that their charge is exactly $e^\bullet = e/m$.

Conclusions

These lecture notes have considered only a few selected aspects of the experiments and theoretical models of the IQHE and the FQHE. The form of presentation might mislead the reader to assume that these phenomena are well understood. This is far from being true, beginning with theoretical models for the FQHE which are radically different from the model presented here. And even within this model important questions remain to be answered : What is the groundstate for $\nu = p/q$ where $p \neq 1$ and $p \neq q = 1$? Hierarchical models have been suggested, where e.g., the quasi-particle of the $\nu = 1/3$ state performs a correlated motion and generates the $\nu = 2/7$ and $\nu = 3/5$ state. A wavefunction as aesthetically appealing as Eq. 14 has not been found yet. Maybe a simple expression does not exist. How do the plateaus in ρ_{xy} and

minima in ρ_{xx} in the FQHE come about? In analogy to the IQHE, localization of particles (quasi-particles in this case) is probably involved. But other scenarios, like the formation of Wigner lattices of quasi-particles, are also being cited. What is the effect of localization on the size of the quasi-particle energy gap? What is the dispersion relation for quasi-particle?... to pose but a few questions.

The experimental data on the new groundstate are also rather rudimentary. Only electrical transport measurements have so far been performed, and the information gained does not go much beyond what can be read off from Fig. 7. The field is wide open for ingenious, though probably difficult, experiments to probe the nature of the electronic state underlying the FQHE and in general to investigate the rich pattern of behavior of a 2D electron system in the presence and absence of a magnetic field over a wide range of carrier densities.

Acknowledgement

Most of the experimental work described in this paper results from a collaboration with D.C. TSUI, A.M. CHANG, P. BERGLUND, G.S. BOEBINGER, J.C.M. HWANG, A.C. GOSSARD, M.A. PAALANEN, J.S. BROOKS and M.J. NAUGHTON, whom I would like to thank for their cooperation and many stimulating discussions. I also benefited immensely from discussions with R.B. LAUGHLIN, B.I. HALPERIN, M. SCHLUTER and P. LITTLEWOOD. I would like to thank K. BALDWIN, W. WIEGMANN and T. BREMAN for excellent technical support.

References

For these lecture notes no attempt is being made to present a complete listing of citations. We would rather refer the reader to several recent reviews and lectures listed at the end.

1. K. von Klitzing, G. Dorda, M. Pepper : Phys. Rev. B28, 4886 (1983)
2. D.C. Tsui, H.L. Störmer, A.C. Gossard : Phys. Rev. Lett. 48, 1559 (1982)
3. H.L. Störmer : Festkörperprobleme XXIV - Advances in Solid State Physics, ed. by P. Grosse (Vieweg, Braunschweig 1984) p.25
4. T. Ando, A. Fowler, Stern : Rev. Mod. Phys. 54, 437 (1982)
5. M.A. Paalanen, D.C. Tsui, A.C. Gossard : Phys. Rev. B25, 5566 (1982)
6. R.B. Laughlin, Phys. Rev. B23, 5632 (1981)
7. A.M. Chang, P. Berglund, D.C. Tsui, H.L. Störmer, J.C.M. Hwang : Phys. Rev. Lett. 53, 997 (1984)
8. D. Yoshioka, B.I. Halperin, P.A. Lee : Phys. Rev. Lett. 50, 1219 (1983)
9. R.B. Laughlin : Phys. Rev. Lett. 50, 1395 (1983)
10. B.I. Halperin : Helv. Phys. Acta 56, 75 (1983)

Reviews and Lectures

Refs. [3] and [10] are reviews.

R.B. Laughlin : In "Two-Dimensional Systems, Heterostructures and Superlattices", Springer Ser. Solid-State Sci. Vol. 53, ed. by G. Bauer, F. Kuchar, H. Heinrich, pp. 272 and 279.

D.C. Tsui : Proc. of the 17th Intl. Conf. on the Physics of Semiconductors, S. Francisco 1984, to be published.